



Computed Tomographic and Magnetic Resonance Imaging Features of Oral Melanoma in a Dog

Arim Lee
Seokmin Lee
Hojung Choi
Youngwon Lee*

College of Veterinary Medicine, Research
Institute of Veterinary Medicine,
Chungnam National University, Daejeon
34134, Korea

*Correspondence: lywon@cnu.ac.kr

ORCID

Arim Lee:

<https://orcid.org/0000-0002-3430-6812>

Seokmin Lee:

<https://orcid.org/0000-0002-8338-8519>

Hojung Choi:

<https://orcid.org/0000-0001-7167-0755>

Youngwon Lee:

<https://orcid.org/0000-0003-3207-0989>

Copyright © The Korean Society of Veterinary Clinics

Abstract Oral melanoma is the most common type of oral tumor in dogs. In this report, computed tomography (CT) and magnetic resonance imaging (MRI) were performed to diagnose a right oral pigmented mass in an 8-year-old dog. The oral mass appeared as a homogeneous soft tissue density parenchyma on pre-contrast CT images, and with heterogeneous enhancement on post-contrast images. Bone destruction of the right mandibular body around the mass and mild enlargement of the right mandibular lymph node were also found. On MRI, the bulky oral mass showed mixed hyperintensity and isointensity compared to the adjacent muscle, where irregular hyperintensity on T1-weighted images corresponded to hypointensity on the T2-weighted images. Based on the physical examinations and imaging results, melanoma was suspected and confirmed via fine-needle aspiration. These unique MRI signals were due to the high paramagnetic melanin content in the tumor, therefore MRI examination could be useful for diagnosis of melanoma.

Key words oral melanoma, computed tomography, magnetic resonance imaging, dog.

Received September 6, 2023 / Revised September 27, 2023 / Accepted September 30, 2023



This is an open access article distributed under the terms of the Creative Commons Attribution Non-Commercial License (<http://creativecommons.org/licenses/by-nc/4.0>) which permits unrestricted non-commercial use, distribution, and reproduction in any medium, provided the original work is properly cited.

Introduction

Melanoma develops from melanocytes and is commonly reported in humans and many animals including dogs and cats (6,13,14). Oral melanoma is the most common type of oral cancer in dogs and accounts for about 7% of all malignant tumors (16). Melanoma can occur anywhere in the oral cavity, but the gingival mucosa is the most common site (12,17). It has a poor prognosis due to local invasion of the surrounding bones such as the mandible and maxilla, and a high rate of metastasis to the surrounding lymph nodes or distant organs (10,15,19). Treatment of oral melanoma includes surgical removal, radiation therapy, anticancer, and immunotherapy (1). Appropriate treatment can be planned and an assessment of the prognosis of melanoma is possible with accurate diagnosis and clinical staging.

Various imaging techniques aid in the diagnosis of oral melanoma. A radiographic examination of the head is not very useful for diagnosis due to the presence of several overlapping structures. Previous studies have reported the features of oral melanoma on computed tomography (CT). These include large size, bone invasions such as osteolysis, a heterogeneous contrast enhancement pattern, and ipsilateral lymphadenopathy (2,9). There are few reports that have described the findings of magnetic resonance imaging (MRI) of oral melanoma in dogs. This case report describes the detailed findings of a dog with oral melanoma, through CT and MRI and discusses the significant features.

Case Report

An 8-year-old male mongrel dog, weighing 13 kg, presented with a right oral pigmented mass. This patient was a stray dog, hence it was hard to obtain an accurate history. Physical examination revealed a dark-colored, firm, movable mass with pain and bleeding, 5 cm in diameter on the labial aspect of the right oral cavity.

Radiographic imaging revealed a round-shaped mass of soft tissue opacity at the level of the right zygomatic arch. However, it was difficult to make a clear evaluation due to the superimposing surrounding structures (Fig. 1A).

Skull and thoracic CT examinations (Alexion™, Canon Medical Systems, Japan) were performed to evaluate the structure, lymph node involvement, and distant metastasis of the oral mass. The patient was positioned in sternal recumbency under general anesthesia. Anesthesia was induced with propofol at a dose of 6 mg/kg administered intravenously and maintained with isoflurane in oxygen. The CT parameters were 120 kilovoltage peak, 150 milliamperes seconds, 1.0 mm

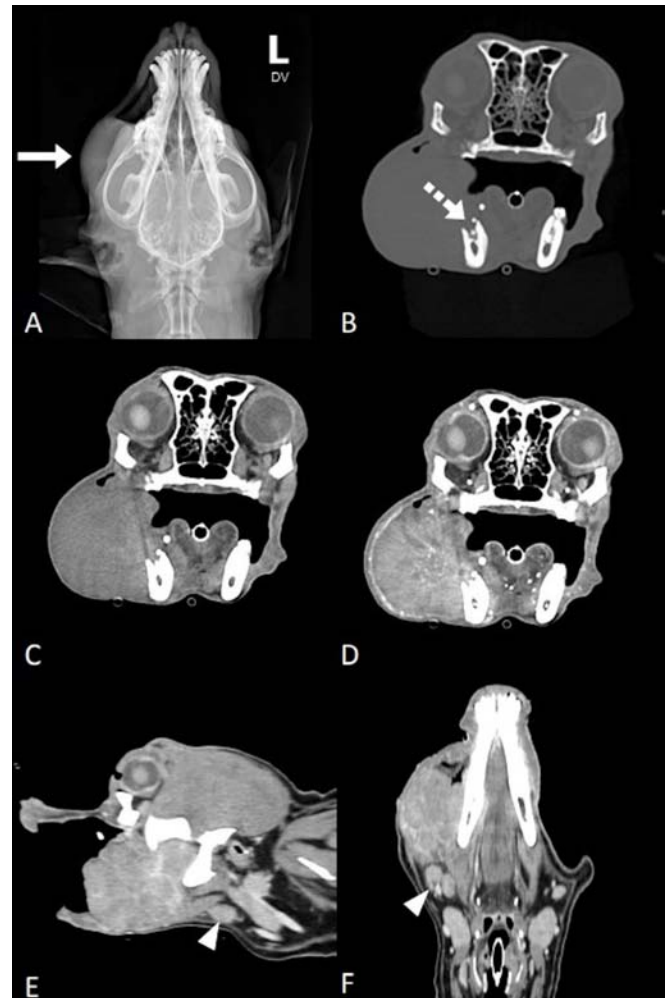


Fig. 1. Dorsoventral radiographs (A) of the head of the dog. The round-shaped mass of soft tissue density is shown at the level of the right zygomatic arch (arrow). CT images of the skull; bone window (B), pre- (C), and post-contrast (D) images of the head at the 1st molar level. Parasagittal (E) and dorsal (F) soft tissue window images at the right mandibular lymph node level. Bone destruction, adjacent to the mass is observed at the dorsal aspect of the right mandibular body at the lower 4th premolar to 1st molar level (B, white dot arrow). The mass shows homogeneous soft tissue density on the pre-contrast images with heterogeneous enhancement on the post-contrast images and extends into the oral cavity (C, D). The right mandibular lymph node (white arrowhead) is mildly enlarged compared to the left side (E, F).

slice thickness, 1.0 mm interval, 0.75 second rotation time, and 0.938 collimation beam pitch. Post-contrast CT images were acquired at 7 and 90 seconds after intravenous injection of 600 mg iodine/kg iohexol (Omnipaque™, GE Healthcare, Ireland). The sagittal and dorsal reconstruction images in the bone and soft tissue window were acquired. The oral mass was huge and filled the right buccal area, with some protrusion into the oral cavity. On the soft tissue window, the

parenchyma of the mass showed a homogeneous soft tissue density on the pre-contrast images with heterogeneous enhancement on the post-contrast images (Fig. 1C, D). But the mass does not appear to have clear differentiation from the surrounding soft tissues. Bone destruction was observed at the dorsal aspect of the right mandibular body at the lower 4th premolar to 1st molar level, around the mass, on the bone window (Fig. 1B). Medial displacement of the right lower 1st molar was also detected. The right mandibular lymph node was mildly enlarged compared to the left side (Fig. 1E, F). In addition, numerous miliary nodules were observed in the overall lung parenchyma, leading to a suspicion of pulmonary metastasis.

MR imaging (1.5 Tesla unit, Vantage Elan™, Canon Medical Systems, Japan) was performed after the CT examination. The dog was scanned with a 16-channel, medium-size coil (1.5 T Receive-Only 16-channel Flex SPEEDER Medium, Canon Medical Systems, Japan). An intravenous injection of 0.5 mmol/mL gadoteric acid (Clariscan™, GE Healthcare AS, Oslo, Norway) at a dose of 0.2 mL/kg was administered. The T1-weighted, T2-weighted, and T2-weighted-fluid-attenuated inversion recovery (T2-FLAIR) and contrast enhanced T1-weighted images were obtained. The oral mass showed a mixed signal of hyperintensity and isointensity compared to the surrounding muscle on the T1-weighted, T2-weighted, and T2-FLAIR images. However, some regions within the mass appeared with irregular hyperintensity on the T1-weighted images and hypointensity on the T2-weighted images (Fig. 2). The post-contrast T1-weighted images showed an overall heterogeneous enhancement.

Fine needle aspiration was performed, and many cells having black-green melanin granules were observed. Based on the cytology, the lesion was tentatively diagnosed as malignant melanoma. Given the huge size and lung metastasis, this patient was classified as stage IV melanoma (19). The prognosis was considered to be poor, and no further treatment was given.

Discussion

There are several reports on the identifying features of oral tumors on CT scans in veterinary medicine, with melanoma accounting for many cases. Malignant oral tumors, including oral melanoma, exhibit several noteworthy features on CT, such as their substantial size, a heterogeneous contrast enhancement pattern, bone lysis, tooth loss, and displacement, invasion of the nasal or oral cavity, and the presence of ipsilateral lymphadenopathy (2,9). All these distinct CT imaging features of malignant oral tumors were manifested in the current case.

In contrast to CT findings, MRI features of oral tumors have been rarely reported. One study described various aspects of signal intensity and contrast enhancement on MRI, along with apparently observed soft tissue margins, for several oral tumors like osteosarcoma and squamous cell carcinoma (7). However, this study did not include cases of oral melanoma, making comparative evaluation difficult.

For dogs, the MRI features of oral melanoma remain unknown, but other melanoma cases such as uveal melanocytoma, and meningeal melanomatosis have been document-

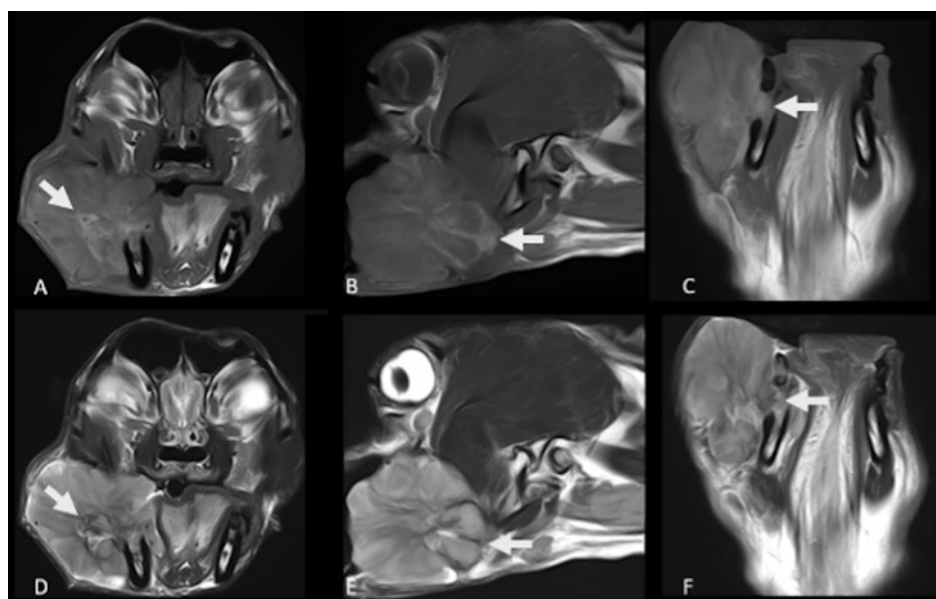


Fig. 2. Transverse (A, D), sagittal (B, E), and dorsal (C, F) planes of T1-weighted (A-C) and T2-weighted MR images (D-F) of the head. The oral mass shows a mixed signal of hyperintensity and isointensity compared to the surrounding muscle. However, some regions show irregular hyperintensity on the T1-weighted images and hypointensity on the T2-weighted images (arrow).

ed. In the case of uveal melanocytoma, the lesion showed hyperintensity on the T1-weighted image and hypointensity on the T2-weighted image (21). The MRI findings of the meningeal melanomatosis generally showed hyperintensity on the T1- and T2-weighted images and hypointense spots on the T2-weighted image in a few small areas (20). On post-contrast T1-weighted images, the lesion was strongly enhanced (20).

In humans, the typical MRI features of melanoma, as obtained from previous reports, involve hyperintensity on the T1-weighted image and hypointensity on the T2-weighted image (5,18). These MRI features stem from the paramagnetic properties of melanin, which has a high affinity for metal ions and acts as a scavenger of organic free radicals (3). These effects shorten the T1 and T2 values and thus cause the unique MRI signals of melanoma (11).

In addition to these characteristic signal patterns, various other patterns have been delineated in humans based on the melanin content of the tumors (8). These comprise lesions exhibiting the following: hypo- to isointensity on the T1-weighted images and iso- to hyperintensity on the T2-weighted images in amelanotic melanoma (4), hyperintensity on both the T1- and T2-weighted images, as well as lesions displaying mixed MRI signals. Furthermore, the presence of methemoglobin due to internal hemorrhaging can induce a range of MRI signal patterns, including iso- to hyperintensity on the T2-weighted images (11). As such, the imaging characteristics of melanoma are so variable that it is impossible to distinguish the pathology with image. That's why histopathological examination must always accompany the process.

In the current case, the MRI findings in some regions correlated with the previously reported MRI characteristics of melanoma. Nevertheless, the overall parenchyma exhibited a pattern demonstrating heterogeneous signals, characterized by a mix of areas of hyperintensity and isointensity. These observations appear to indicate variations in internal melanin concentration and bleeding.

The mass were detected using both imaging modalities. As anticipated, the soft tissue boundaries were better visible on MR images, or the margin of the mass was more evident MR images. So MRI will be helpful when formulating treatment plans such as surgery and radiation therapy.

Conclusions

The possibility of oral melanoma should be considered if the CT findings of malignant oral tumors such as bone infiltration, heterogeneous contrast enhancement, and lymph node metastatic findings and MRI features of hyperintensity

on the T1-weighted images and hypointensity or isointensity on T2-weighted images are seen. Although melanoma could appear with varying intensities on the MRI, it is considered that MR imaging will be very useful for the differential diagnosis of melanoma if the mass shows signals that are specific for melanoma (T1 hyperintensity and T2 hypointensity). More experience is needed to establish diagnostic imaging parameters that can confirm the diagnosis using MR imaging in canine oral melanoma.

Conflicts of Interest

The authors have no conflicting interests.

References

1. Bergman PJ. Canine oral melanoma. *Clin Tech Small Anim Pract* 2007; 22: 55-60.
2. Choisunirachon N, Lin LS, Tanaka Y, Saeki K, Fujiwara R, Nishimura R, et al. Retrospective study of computed tomographic characterization of canine oral malignant melanoma in 24 dogs. *Thai J Vet Med* 2014; 44: 497-503.
3. Felix CC, Hyde JS, Sarna T, Sealy RC. Interactions of melanin with metal ions. Electron spin resonance evidence for chelate complexes of metal ions with free radicals. *J Am Chem Soc* 1978; 100: 3922-3926.
4. Gunbey HP, Gunbey E, Sayit AT, Aslan K. Magnetic resonance imaging (MRI) appearances of primary amelanotic malign melanoma in the nasal cavity: a rare case. *J Clin Diagn Res* 2015; 9: TD01-TD03.
5. Hayashi T, Ito J, Katsura K, Honma K, Shingaki S, Ikarashi T, et al. Malignant melanoma of mandibular gingiva; the usefulness of fat-saturated MRI. *Dentomaxillofac Radiol* 2002; 31: 151-153.
6. Houghton AN, Polsky D. Focus on melanoma. *Cancer Cell* 2002; 2: 275-278.
7. Kafka UC, Carstens A, Steenkamp G, Symington H. Diagnostic value of magnetic resonance imaging and computed tomography for oral masses in dogs. *J S Afr Vet Assoc* 2004; 75: 163-168.
8. Lee PH, Wang LC, Lee EJ. Primary intracranial melanoma. *J Cancer Res Pract* 2017; 4: 23-26.
9. Lee S, Jang Y, Lee G, Jeon S, Kim D, Choi J. CT features of malignant and benign oral tumors in 28 dogs. *Vet Radiol Ultrasound* 2021; 62: 549-556.
10. Liptak JM, Withrow SJ, Selting KA, Turek MM. Cancer of the gastrointestinal tract. In: Withrow SJ, Vail DM, Page RL, editors. *Withrow and MacEwen's small animal clinical oncology*. 5th ed. St. Louis: Elsevier/Saunders. 2013: 381-395.
11. Marx HF, Colletti PM, Raval JK, Boswell WD Jr, Zee CS. Magnetic resonance imaging features in melanoma. *Magn Reson Imaging*

- 1990; 8: 223-229.
12. McEntee MC. Clinical behavior of nonodontogenic tumors. In: Verstraete FJM, Lommer MJ, editors. Oral and maxillofacial surgery in dogs and cats. Philadelphia: Saunders. 2012: 387-402.
 13. Nishiya AT, Massoco CO, Felizzola CR, Perlmann E, Batschinski K, Tedardi MV, et al. Comparative aspects of canine melanoma. *Vet Sci* 2016; 3: 7.
 14. Patnaik AK, Mooney S. Feline melanoma: a comparative study of ocular, oral, and dermal neoplasms. *Vet Pathol* 1988; 25: 105-112.
 15. Ramos-Vara JA, Beissenherz ME, Miller MA, Johnson GC, Pace LW, Fard A, et al. Retrospective study of 338 canine oral melanomas with clinical, histologic, and immunohistochemical review of 129 cases. *Vet Pathol* 2000; 37: 597-608.
 16. Smith SH, Goldschmidt MH, McManus PM. A comparative review of melanocytic neoplasms. *Vet Pathol* 2002; 39: 651-678.
 17. Todoroff RJ, Brodey RS. Oral and pharyngeal neoplasia in the dog: a retrospective survey of 361 cases. *J Am Vet Med Assoc* 1979; 175: 567-571.
 18. Uchiyama Y, Murakami S, Kawai T, Ishida T, Fuchihata H. Primary malignant melanoma in the oral mucosal membrane with metastasis in the cervical lymph node: MR appearance. *AJNR Am J Neuroradiol* 1998; 19: 954-955.
 19. Williams LE, Packer RA. Association between lymph node size and metastasis in dogs with oral malignant melanoma: 100 cases (1987-2001). *J Am Vet Med Assoc* 2003; 222: 1234-1236.
 20. Wu CC, Huang WH, Liao PW, Chang YP. Diagnosis of meningeal melanomatosis in a dog using magnetic resonance imaging and cerebrospinal fluid findings. *J Vet Med Sci* 2021; 83: 94-99.
 21. Yoon H, Yu J, An T, Lee H, Kim H, Kim D, et al. Magnetic resonance findings of a canine benign uveal melanocytoma. *J Vet Clin* 2018; 35: 233-236.